25th ABCM International Congress of Mechanical Engineering
October 20-25, 2019, Uberlândia, MG, Brazil

COB-2019-2057
ANALYSIS OF NUMERICAL METHODS FOR 1D COMPRESSIBLE UNSTEADY FLOW IN ENGINE APPLICATION

Felipe Augusto Ferreira Gomes
Waldyr Luiz Ribeiro Gallo
University of Campinas - Cidade Universitária Zeferino Vaz - Barão Geraldo, Campinas - SP, 13083-970
f.augustofgomes@gmail.com
gallo@fem.unicamp.br

Abstract. *The flow characteristics inside intake and exhaust manifolds direct influence engine performance and a model capable of estimating its behavior becomes essential. Among the numerical methods, the inviscid one-dimensional (1D) approach has shown to be a suitable approximation for the problem. The method of characteristics (MC), which has first order accuracy, was the first method to be applied to gas motion inside engine manifolds with reliable results. Another widely used method is the two step of Lax-Wendroff (LW2), which has second order accuracy on smooth regions of the flow. The literature indicates that both methods presented similar results regarding engine performance. For this reason, two different approaches for MC; the classical method (MC-Winterbone) and the modification made by Payri (MC-Payri), and LW2 were implemented and compared with each other and against the open-source software OpenWAM^{TM} in a tapered pipe simulation. For unsteady state study, all methods showed good agreement for pressure and velocity variation, with more notably divergences on velocity. For steady state analysis, two investigations were undertaken; mean mass flow rate precision and mass flow rate consistency with its mean value. It was shown that MC-Payri improved the mass conservation and the quality of the estimated properties when compared to MC-Winterbone. OpenWAM-TVD scheme displayed the best results but the LW2 implemented in this work presented superior consistency. This is probably due to the different treatment used by OpenWAM^{TM} at the boundaries.*

Keywords: *1D gas dynamics, tapered pipe, method of characteristics, two step Lax-Wendroff*

1. INTRODUCTION

The gas exchange systems of an engine heavily contributes to its performance. It affects the flow motion inside the manifolds which in turn influences volumetric efficiency. Therefore, a precise modeling of the unsteady compressible flow inside the manifolds enables a more accurate analysis of the engine performance. Mostly nowadays engines run in four-stroke cycles with poppet valves in which the gas exchange is divided in intake and exhaust processes. Regarding numerical models, the influence of intake and exhaust systems on engine performance have been accounted by basically three approaches: quasi-steady, filling and emptying and wave action (Benson, 1982). Quasi-steady models assume constant gas properties and rely on empirical data. Filling and emptying approach corresponds to zero dimensional models applied to a finite volume. It takes into account the unsteady behavior of the flow but considers the gas properties homogeneous throughout the volume. Additionally, it is still vastly used to estimate the operation of engine systems such as the cylinder and plenum.

Wave action approach consists of dimensional models of the unsteady compressible flow inside the intake and exhaust systems. Although 3D models give theoretically more accurate results about the flow field, they are very computationally expensive and time demanding. Their use is more common analyzing complex junctions and subparts of the system, such as valves. One-dimensional (1D) models have presented the most success despite of its simplifications. They have shown good agreement with experimental data and relative low computational cost (Winterbone and Pearson, 2000). However, these models encounter limitations in the presence of more complex geometries and apparatus such as valves, throttle bodies, multi pipe junctions and sudden area change in which multidimensional effects cannot be ignored. Correlations and approximated methods have been developed for the 1D models taking into account those effects, however, many of them require experimental data (Winterbone and Pearson, 2000).

1.1 Methods applied to engine manifolds

Benson *et al.* (1964) was one of the first to apply computational one-dimensional models to engine manifold systems. They developed a mesh method of characteristics, which was based on the graphical technique of the method. This method

became the most used for geometrical studies of intake and exhaust systems until the decade of 1990. It is still relevant to this day because of its applicability on boundary conditions. The numerical method of characteristics as well as the graphical solution are well developed in Benson (1982).

In the mid 80's, finite difference and finite volume schemes started to be extensively used. The two step Lax-Wendroff and MacCormack schemes were the most employed on engine performance and even noise prediction (Payri *et al.*, 1996). Even though both schemes demonstrated to be faster than the mesh method of characteristics, they presented spurious oscillations when faced with discontinuities such as shock waves and contact surfaces. The presence of non-physical overshooting may be overcome by employing flux limiting schemes. They usually consists of flux corrector techniques (FCT) or total variation diminishing (TVD) schemes.

In the last decade, the 1D-3D model have been introduced. It couples a one-dimensional solver with a three-dimensional one. This model has shown to overcome the limits of 1D models on simulating complex geometries. It has been accurately use to predict noise while solving engine performance parameters (Montenegro *et al.*, 2016). This model has been included in many commercial software and it is still being improved (Della Torre *et al.*, 2017).

The present work consists of testing multiple numerical schemes for the flow inside engine manifolds systems, accounting for its accuracy and numerical consistency. At the boundaries, the method of characteristics was employed and an investigation regarding the more appropriate approach was made.

2. METHODOLOGY

The two step Lax-Wendroff scheme (LW2) and two different approaches for the method of characteristics (MC), classical approach and the modification made by Payri *et al.* (1986), were implemented in MATLAB and tested against the open source software OpenWAM^{TM}.

2.1 Governing Equations

The governing equations for an inviscid 1D compressible unsteady flow with area variation are characterized as non-linear hyperbolic partial differential equations, which may be expressed in conservation law form, Eq. (1), or non-conservation law form, Eq. (2), as indicated by Toro (1999).

$$\frac{\partial}{\partial t}\begin{bmatrix}\rho F\\ \rho u F\\ \rho e_0 F\end{bmatrix}+\frac{\partial}{\partial x}\begin{bmatrix}\rho u F\\ \left(\rho u^2+p\right)F\\ \rho u h_0 F\end{bmatrix}+\begin{bmatrix}0\\ -p\frac{dF}{dx}+g\rho F_l\\ -q\rho F\end{bmatrix}=0 \qquad \text{or} \qquad \frac{\partial \mathbf{U}}{\partial t}+\frac{\partial \mathbf{F(U)}}{\partial x}+\mathbf{C(U)}=0 \tag{1}$$

$$\begin{cases}\dfrac{\partial \rho}{\partial t}+u\dfrac{\partial \rho}{\partial x}+\rho\dfrac{\partial u}{\partial x}+\dfrac{\rho u}{F}\dfrac{\partial F}{\partial x}=0\\ \dfrac{\partial u}{\partial t}+u\dfrac{\partial u}{\partial x}+\dfrac{1}{\rho}\dfrac{\partial p}{\partial x}+g\dfrac{F_l}{F}=0\\ \dfrac{\partial e}{\partial t}+u\dfrac{\partial e}{\partial x}-\dfrac{p}{\rho^2}\left[\dfrac{\partial \rho}{\partial t}+u\dfrac{\partial \rho}{\partial x}\right]-\left(q+ug\dfrac{F_l}{F}\right)=0\end{cases} \tag{2}$$

Where F is the area, F_l is area per unit of length, q is the heat transfer rate through walls, $g=\frac{1}{2}C_f u|u|$ is the wall friction factor, ρ is density, u is flow velocity, p is pressure, e_0 is the total specific internal energy and h_0 is stagnation enthalpy. The perfect gas relations are used to close the system of equation.

2.2 Numerical Solution

The solution for MC is derived from the non-conservation law form and it is usually expressed in terms of non-dimensional Riemann variables, $\lambda = A + U(k-1)/2$ and $\beta = A - U(k-1)/2$, and entropy level, A_A, where A is the non-dimensional speed of sound. Its solution consists of reducing the set of three partial differential equations (PDE) into a set of three ordinary differential equations (ODE) with solution along specific curves called characteristics, the three ODEs are given in Eq. (3) to Eq. (5) and are called compatibility equations (Winterbone and Pearson, 2000).

Figure (1) (a) illustrates the three point stencil used in the MC, to estimate the solution at time level $n+1$ for i the method of Euler is employed. However, it is necessary to identify the values of the properties at points L, K and R. The classical approach, named in this work MC-Winterbone, calculates the properties in mid-mesh points by linear interpolation of the λ, β and A_A. Nonetheless, Payri *et al.* (1986) argues that the linear interpolation of the Riemann variables promotes errors for pipes with variable cross section area. Thus, they recommend the linear interpolation of volumetric flow and static pressure instead. Both approaches are relevant for the use at the boundaries since partial information of the flow can be estimated, as explained in the next section. In the case of LW2 simulations, the interpolations were done using Payri's approach.

$$\left.\frac{dA_A}{dZ}\right|_K = \frac{k-1}{2}\frac{A_A}{A^2}\left[q\frac{L_{ref}}{a_{ref}^3} + Ug\frac{F_l}{F}\frac{L_{ref}}{a_{ref}^2}\right] \tag{3}$$

$$\left.\frac{d\lambda}{dZ}\right|_L = \frac{A}{A_A}\frac{dA_A}{dZ} - \frac{k-1}{2}g\frac{F_l}{F}\left[1-(k-1)\frac{U}{A}\right]\frac{L_{ref}}{a_{ref}^2} + \frac{(k-1)^2}{2}\frac{q}{A}\frac{L_{ref}}{a_{ref}} - \frac{k-1}{2}\frac{UA}{F}\frac{dF}{dX} \tag{4}$$

$$\left.\frac{d\beta}{dZ}\right|_R = \frac{A}{A_A}\frac{dA_A}{dZ} - \frac{k-1}{2}g\frac{F_l}{F}\left[-1-(k-1)\frac{U}{A}\right]\frac{L_{ref}}{a_{ref}^2} + \frac{(k-1)^2}{2}\frac{q}{A}\frac{L_{ref}}{a_{ref}} - \frac{k-1}{2}\frac{UA}{F}\frac{dF}{dX} \tag{5}$$

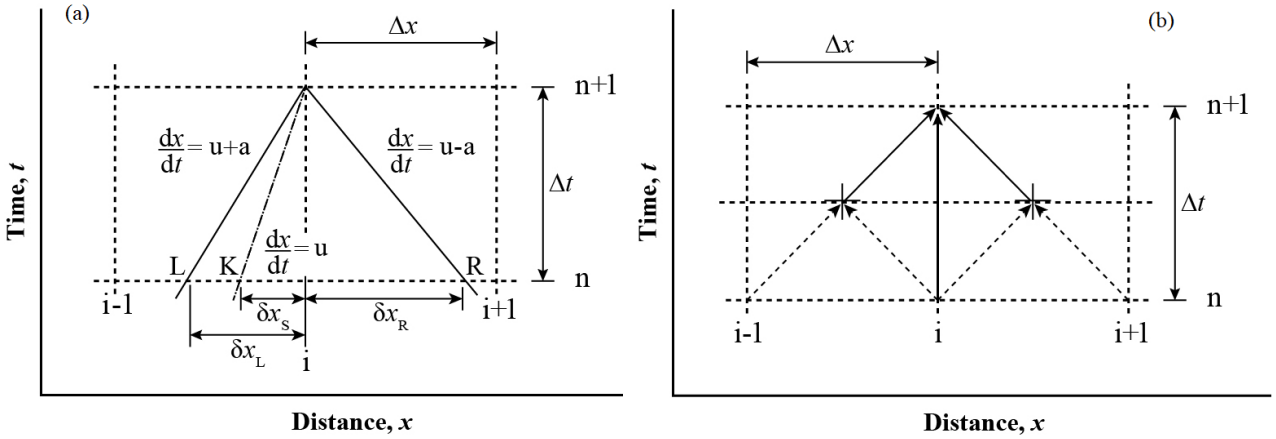

Figure 1. (a) Method of characteristics mesh grid for subsonic flow, (b) Two step Lax-Wendroff mesh grid

The last implemented method was the two step Lax-Wendroff (LW2), which is a centered based scheme with second order accuracy in which it is divided in two steps applied on half time mesh grid. The scheme uses the conservation law form with a three point stencil around i, as shown in Fig. (1) (b). The first step is calculated by Eq. (6) and Eq. (7) which uses information from $i-1$, i, and $i+1$. Then, the second step uses the quantities estimated in the first step plus the values of i at time level n to finally obtain $\mathbf{U}_i^{n+1}$ using Eq. (8).

$$\mathbf{U}_{i-1/2}^{n+1/2} = \frac{1}{2}\left(\mathbf{U}_i^n + \mathbf{U}_{i-1}^n\right) - \frac{\Delta t}{2\Delta x}\left(\mathbf{F}_i^n - \mathbf{F}_{i-1}^n\right) - \frac{\Delta t}{4}\left(\mathbf{C}_i^n + \mathbf{C}_{i-1}^n\right) \tag{6}$$

$$\mathbf{U}_{i+1/2}^{n+1/2} = \frac{1}{2}\left(\mathbf{U}_i^n + \mathbf{U}_{i+1}^n\right) - \frac{\Delta t}{2\Delta x}\left(\mathbf{F}_{i+1}^n - \mathbf{F}_i^n\right) - \frac{\Delta t}{4}\left(\mathbf{C}_i^n + \mathbf{C}_{i+1}^n\right) \tag{7}$$

$$\mathbf{U}_i^{n+1} = \mathbf{U}_i^n - \frac{\Delta t}{\Delta x}\left(\mathbf{F}_{i+1/2}^{n+1/2} - \mathbf{F}_{i-1/2}^{n+1/2}\right) - \frac{\Delta t}{2}\left(\mathbf{C}_{i+1/2}^{n+1/2} + \mathbf{C}_{i-1/2}^{n+1/2}\right) \tag{8}$$

2.3 Boundary conditions

None of the methods are able to fully estimate the flow behavior at the end of the pipes, the boundaries, because information from outside of the pipe is necessary. Winterbone and Pearson (2000) state that the best way to incorporate the boundary with the wave models is by the Method of Characteristics. They argue that it gives better physical insight since the wave can be followed until the end of the pipe along the characteristic curves. The boundaries used in this work were based on the approach given by Benson (1982).

At the boundaries is assumed to have a quasi-steady flow. This implies that the size of the boundary is too small compared with the length of the pipe connected to it. This also suggests that at the boundary any property have much larger spatial rate of change than rate of change with regards to time, $\partial/\partial x \gg \partial/\partial t$. Applying only the quasi-steady equations of continuity, momentum and energy on a boundary usually creates an indeterminate system of equations

(Winterbone and Pearson, 2000). The compatibility equations of the method of characteristics are then required to find a solvable set of equations.

The Riemann variables are generalized when applied to boundary equations. Here, they will be call incident wave, λ_{in}, for the wave approaching the boundary and reflected wave, λ_{out}, for the one leaving the boundary. In case of flow going into the pipe (inflow), the entropy level and the incident wave are corrected as indicated by Benson (1982).

The only boundary condition used in this work was an open end. It is necessary to investigate inflow and outflow, both with subsonic and sonic velocities. For an open end with subsonic flow going out of the pipe, it is assumed that the pressure at the end of the pipe is equal to the outside pressure, p_0. This implies that there is no pressure loss between the last point of the pipe and the external environment. A relation for the reflected wave can then be derived as Eq. (9).

$$\lambda_{out} = 2A_A \left(\frac{p_0}{p_{ref}} \right)^{(k-1)/2k} - \lambda_{in} \tag{9}$$

For sonic flow, $A = U$, the reflected wave is estimated as Eq. (10):

$$\lambda_{out} = \lambda_{in} \left(\frac{k-3}{k+1} \right) \tag{10}$$

In the instance of inflow, it is assumed an isentropic change from the outside condition, at A_0 and p_0, into the pipe, at A and p. Applying the energy equation with the incident wave for the boundary leads to the quadratic equation of U in Eq. (11) in which the positive root gives the appropriate physical result.

$$U^2 \left[\left(\frac{k-1}{2} \right)^2 + \left(\frac{A_{A_n}}{A_A} \right)^2 \right] - U(k-1)\lambda_n + \lambda_n^2 - A_0^2 \left(\frac{A_{A_n}}{A_A} \right)^2 = 0 \tag{11}$$

From the value of U, the non-dimensional speed of sound can be determined by the energy equation and, at last, both Riemann variables from their definition.

The system of equations just described accept flow velocity reaching supersonic levels. However, in reality, the flow would chock and the inflow velocity would be sonic, $U = A$. Applying this condition yields Eq. (12).

$$A = U = \sqrt{\frac{2}{k+1}} A_0 \tag{12}$$

2.4 Simulations

The spacial mesh is evenly spaced, Δx constant, while the time step changes every iteration according the Courant–Friedrichs–Lewy (CFL) stability criterion, CFL ≤ 1. It can be expressed in Eq. (13), where c^n_{max} represents the greatest wave speed at time level n in the whole numerical domain.

$$dt = \text{CFL} \frac{dx}{c^n_{max}} \tag{13}$$

The numerical methods were tested for a tapered pipe using the scheme proposed by Liu *et al.* (1996), Fig. (2) (a). The test consists of a convergent pipe, with 50 mm diameter on one end and 10 mm in the opposite end. The smallest end is connected to the atmospheric conditions while the opposite end is connected to a chamber of constant pressure and temperature. At the beginning, the fluid inside the pipe, which is stationary at atmosphere conditions, is separated from the chamber by a diaphragm. At time $t = 0$, the diaphragm breaks and fluid starts to flow through the pipe until it reaches steady state. The simulation condition is summarized in Fig. (2) (b). The three implemented methods were compared to LW2 and TVD scheme from OpenWAM$^{\text{TM}}$. The high definition scheme is mostly used as comparative parameter for the other schemes.

3. RESULTS

When the diaphragm is broken, a high compression wave starts to propagate towards the opposite end. The wave increases the local pressure and flow velocity as the cross-section area reduces. Figure (3) illustrates the pressure profile in the pipe after 2 ms for all methods for CFL = 1.0 and 0.9.

(a)

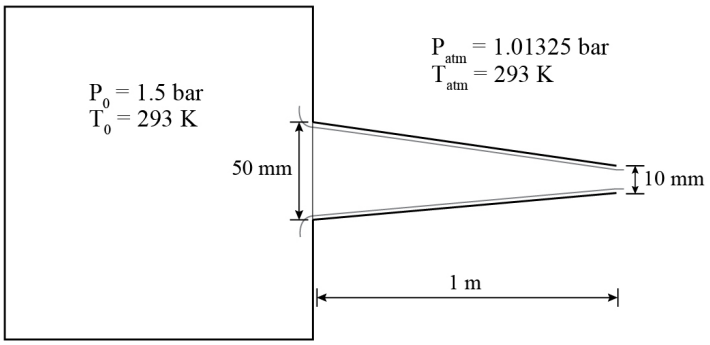

(b)

Characteristics	Value
Pipe length	1.0 m
Diameter entry	50 mm
Diameter exit	10 mm
Mesh length	50 mm
CFL	1.0
Heat Transfer	ignored
Friction	ignored

Figure 2. (a) Tapered pipe connected to a constant pressure and temperature chamber, (b) Characteristics of the simulations

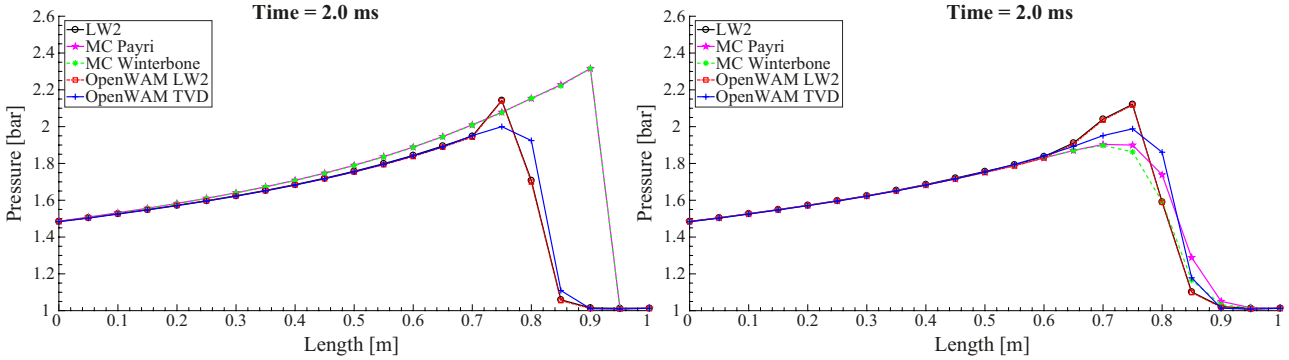

Figure 3. Pressure field inside the tapered pipe with CFL = 1.0 on the left, Pressure field inside the tapered pipe with CFL = 0.9 on the right

For CFL equal unit, the simulated wave by both method of characteristics have shown a much faster propagation compared to the other methods, presenting the pressure peak around 20 cm further than the slowest scheme, the LW2. The TVD was slightly faster than the LW2 by about 5 cm or one mesh length. Reducing the CFL number to 0.9 overcame the disparity observed in wave propagation speed of the MCs, achieving results similar to those of higher order. However, it also smoothed its solution, which removed the capacity to predict the pressure discontinuity accurately. As expected, the LW2 was the only method to present non-physical overshooting. In addition, both LW2 had almost exact results for both CFL number, as did the method of characteristics. Since the results for CFL at 0.9 showed a better agreement, this value was used for all the other simulations.

When the compression wave reaches the open end, it is reflected as a rarefaction wave. Such wave travels back towards the inflow entry, reflecting again with opposite sign. This cycle repeats until the flow reaches steady state.

The pressure and velocity variation with time at both ends of the pipe are described in Fig. (4) and Fig. (5). At the inflow end, Fig. (4), all the methods presented good agreement with each other, specially pressure. It can be noticed that the first rarefaction wave arrived around 6 ms and the second one about 13 ms, with much lower intensity. The simulated velocity for both method of characteristics showed divergences around 5 ms. They also demonstrated greater velocity levels as the flow tends to steady state.

At the smaller end, the pressure becomes higher than atmospheric only for sonic flow due to the conditions imposed in Sec. (2.3). The flow chocked with the arrival of the first high pressure wave and it maintained sonic until 3.5 to 4 ms, depending on the scheme. Both LW2 methods showed the highest pressure peaks, with almost identical values. They were followed by the OpenWAM-TVD, MC-Winterbone and MC-Payri, respectively. The MC-Winterbone was the only method to present more distinct values after the first pressure peak. In fact, it even estimated chocked flow after the arrival of the second high pressure wave, which occurred around 8.5 ms.

In the flow velocity variation, Fig. (5) on the right, it becomes clear that MC-Winterbone estimated the fastest flow as the state moves toward steady. Both LW2 had practically the same qualitative and quantitative results throughout the time range analyzed. The OpenWAM-TVD showed consistently the highest trough along the simulation.

Overall, for the unsteady analysis, the higher order methods presented very similar results of pressure and velocity at both ends of the pipe. The methods of characteristics showed more significant distinction for flow velocity, specially at the 10 ms end. This is probably due to the higher variation from node to node towards the end of the pipe.

The properties of the flow started to present minor changes around 80 ms. To ensure steady state condition, the results

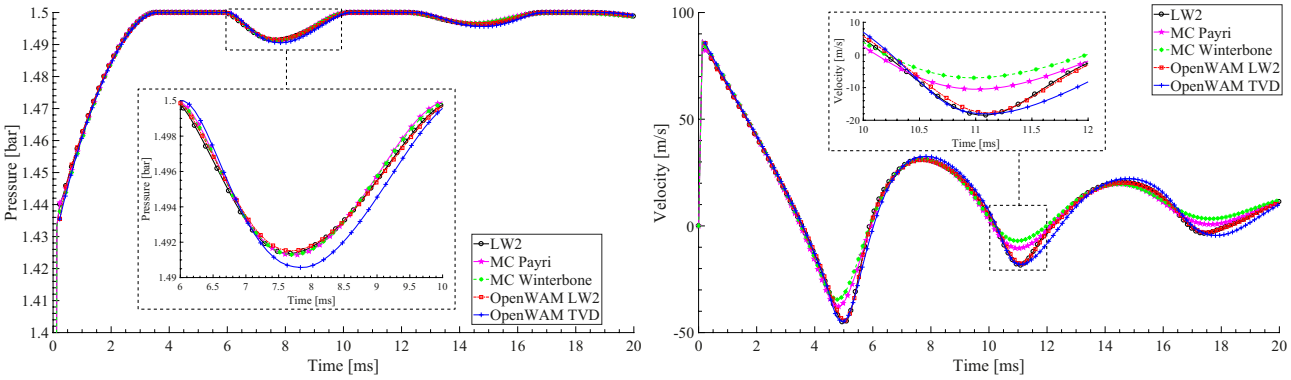

Figure 4. Comparison between the methods at the entry location, x=0 m. Pressure variation on the left and velocity variation on the right

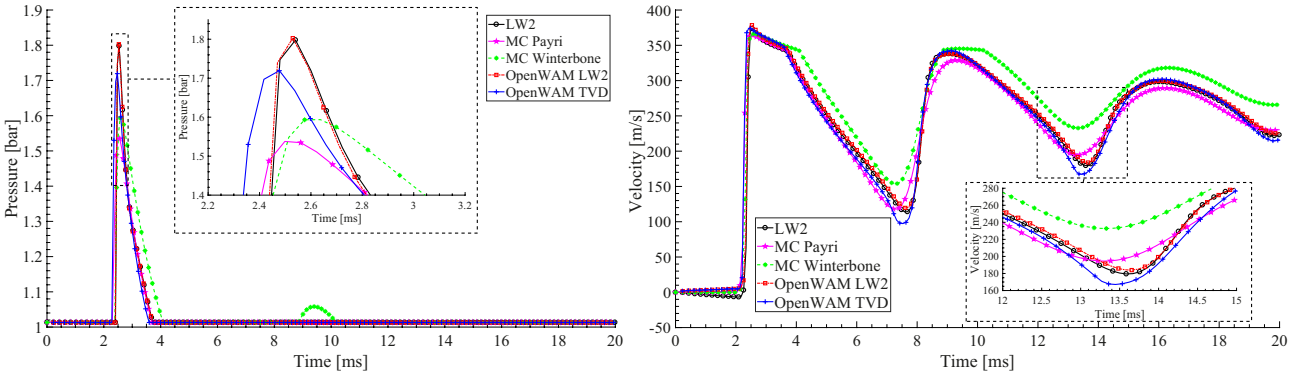

Figure 5. Comparison between the methods at the exit location, x=1 m. Pressure variation on the left and velocity variation on the right

were taken at 500 ms of simulated time. Because the flow is assumed to be isentropic, the stagnation pressure should be constant through the pipe at steady state. Thus, an analytical solution for mass flow rate for subsonic compressible flow can be derived as Eq. (14) as shown in White (2011). The subscript e represents the value at the 10 ms exit while the subscript 0 the properties inside the chamber.

$$\dot{m} = F_e \frac{P_0}{\sqrt{RT_0}} \sqrt{\frac{2k}{k-1}\left(\frac{P_e}{P_0}\right)^{2/k}\left[1-\left(\frac{P_e}{P_0}\right)^{(k-1)/k}\right]} \tag{14}$$

The mass flow error was calculated by comparing the mean values obtained from the numerical schemes with the analytical solution in Eq. (14). Figure (6) illustrates the mass flow rate profile inside the pipe for all schemes.

It is clear that the higher order methods remarkably improved the mass flow rate when compared to the first order methods, all with errors below 5.0 % for a 21 points mesh grid. The two worst performing methods were both method of characteristics. However, MC-Payri significantly improved the mass flow error when compared to the classic approach of the method of characteristics, from 23.38 % to 8.86 %. Both LW2 methods presented similar qualitative and quantitative results. Nonetheless, the mass conservation error from OpenWAM's was more than 1 % higher. The likely cause lies on the fact that OpenWAM^{TM} estimates the incident waves and entropy level by linearly interpolating p, a and u, therefore, it does not take into account any area change. This can also be observed in the OpenWAM-TVD scheme. Where, despite it had the best mass conservation result, it showed diverging values on the first and last mesh points. Therefore, a second analysis was made to study the consistency of the numerical results with its own estimated mean mass flow rate value, where Eq. (15) was used. The results are presented in Tab. (1). It can be seen that LW2 implemented in this work showed the best conservation consistency of all methods. The error given by OpenWAM^{TM} in both its methods were very close, which also suggests that the divergence at the boundary nodes were due to the different interpolating approach in the method of characteristics.

$$\text{error} = \frac{\sum_{i=1}^{N} |\bar{\dot{m}} - \dot{m}_i|}{N\bar{\dot{m}}} \times 100 \tag{15}$$

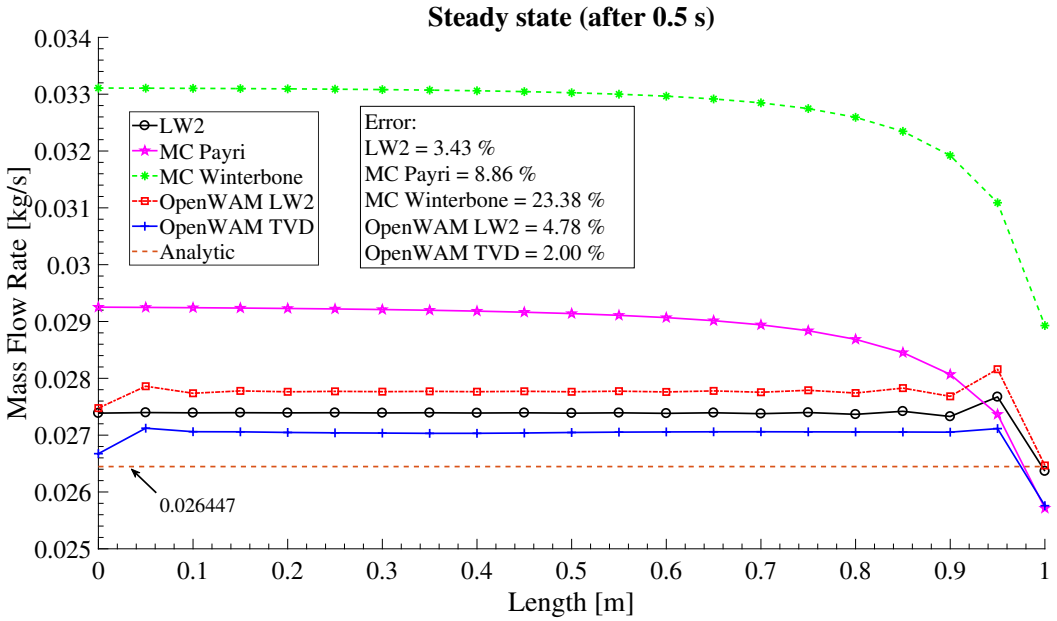

Figure 6. Mass flow profile in steady state for CFL$=0.9$

Table 1. Mass flow error according to Eq. (15)

	MC-Winterbone	MC-Payri	LW2	OpenWAM - LW2	OpenWAM - TVD
error [%]	1.83	1.87	0.35	0.52	0.54

The mass flow at the boundaries of pipes are extremely important for engine simulation because they determine the amount of mass that enters or leave the cylinder during the simulation. For instance, if the above simulation represented a charge into a cylinder through the right boundary, the TVD method would under predict the mass flow while both LW2 would deliver a much more accurate amount of fresh charge. Therefore, the methods have to be accurate and consistent at the boundaries at the same time.

The other conservative quantities such as energy and stagnation pressure had the exactly same distribution form and for that they will not be presented. Overall, the results found agreed with the ones in Liu *et al.* (1996).

At last, it was studied the convergence of the mean mass flow rate with mesh size for the three best performing methods, LW2, OpenWAM-LW2 and OpenWAM-TVD. The analytical solution was used as benchmark for estimating the error. For most cases, OpenWAM-TVD displayed the lowest error, sometimes an order of magnitude lower than the others. For dx=1.0 mm, LW2 found the exact solution with 10^{-6} precision. However, refining the mesh to 0.5 mm showed that the method walks toward an under predicted value of the mass flow rate. After certain level of refinement, 1.0 mm for LW2 and 2.5 mm for TVD, the error experienced more modest variations. The TVD reached an error below 1 % for a mesh size of 25 mm (41 mesh points) while both LW2 methods were able to reach that precision only for dx=10 mm (101 mesh points). This illustrates that even though TVD schemes are more expensive, they may result in less computational time for the same desired precision.

Table 2. Mean mass flow error [%]

dx [mm]	LW2	OpenWAM - LW2	OpenWAM - TVD
50.0	3.4257	4.7832	2.0040
25.0	1.8150	2.0380	0.5407
10.0	0.5067	0.5445	0.0832
5.0	0.1550	0.1777	0.0265
2.5	0.0378	0.0567	0.0151
1.0	0.0000	0.0189	0.0113
0.5	-0.0076	0.0151	0.0113

It is important to mention that for errors below 1 % the difference from the boundary points to the rest of the domain was insignificant. Thus, a very precise method can ensure some level of consistency at the boundaries.

4. CONCLUSION

Three wave capture schemes were implemented in MATLAB; the classic method of characteristics (MC-Winterbone), a modification made by Payri (MC-Payri) and two steps of Lax-Wendroff (LW2). These methods were tested and compared to LW2 and TVD schemes available in the open source software OpenWAM^{TM} in a tapered pipe simulation. Both MC estimated a significant faster wave propagation than the other methods for CFL=1.0 but achieved similar results for CFL=0.9. Thus, CFL=0.9 was used for all the studies made afterwards. In the unsteady flow analysis, all developed method presented similar results for pressure and flow velocity variation. The largest divergences were encountered by MC-Winterbone, in which it estimated a second chocked flow on the right end and overall showed the fastest flow. The second order methods displayed very similar results throughout the simulation. Nonetheless, in the steady state analysis, more notable differences were detected. Since the flow is isentropic, an analytical solution for the steady state flow was used as benchmark. Regarding mass conservation, the higher order methods demonstrated a remarkable enhancement by which the best performing method was the TVD, with 2.0 % error, while the worst was MC-Winterbone, with error above 23 %. However, Payri's modification on the method of characteristics improved mass conservation and quality of mass flow rate results significantly. Therefore, it showed to be the best method to be used at the boundaries for a higher order scheme. The Lax-Wendroff scheme employed in this work improved the mass conservation compared to OpenWAM-LW2 by more than 1 %; probably caused by the different treatment at the boundaries. A mass conservation consistency analysis was undertaken in order to evaluate the discrepancy in each mesh point. The results showed LW2 as the most consistent method, also implying that the difference at the boundaries were caused by the distinct properties interpolation of the method of characteristics. Moreover, it is concluded that the volumetric flow rate is a better parameter to interpolate than flow velocity. The last investigation was done on the convergence of the three best performing methods, LW2 and both OpenWAM^{TM} methods. The TVD found an error below 1 % with 41 mesh points while both LW2 were able to reach this precision only with 101 points. Therefore, a high resolution scheme may result in less computational expense for a specific precision, despite TVD's higher numerical cost. This analysis is recommended for future works.

5. ACKNOWLEDGEMENTS

We would like to thank CAPES for helping this project by funding through a master's scholarship.

6. REFERENCES

Benson, R.S., 1982. *The Thermodynamics and Gas Dynamics of Internal Combustion Engines Volume 1*. Oxford : Clarendon Press.

Benson, R., Garg, R. and Woollatt, D., 1964. "A numerical solution of unsteady flow problems". *International Journal of Mechanical Sciences*, Vol. 6, No. 1, pp. 117–144.

Della Torre, A., Montenegro, G., Cerri, T. and Onorati, A., 2017. "A 1D/Quasi-3D Coupled Model for the Simulation of I.C. Engines: Development and Application of an Automatic Cell-Network Generator". *SAE International Journal of Engines*, Vol. 10, No. 2.

Liu, J., Schorn, N., Schernus, C. and Peng, L., 1996. "Comparison Studies on the Method of Characteristics and Finite Difference Methods for One-Dimensional Gas Flow through IC Engine Manifold". In *SAE International Journal of Engines*. SAE International Journal of Engines, 412.

Montenegro, G., Cerri, T., Della Torre, A., Onorati, A., Fiocco, M. and Borghesi, D., 2016. "Fluid Dynamic Optimization of a Moto3 Engine by Means of 1D and 1D-3D Simulations". *SAE International Journal of Engines*, Vol. 9, No. 1, pp. 2016–01–0570.

Payri, F., Corberán, J.M. and Boada, F., 1986. "Modifications to the Method of Characteristics for the Analysis of the Gas Exchange Process in Internal Combustion Engines". *Proceedings of the Institution of Mechanical Engineers, Part D: Transport Engineering*, Vol. 200, No. 4, pp. 259–266.

Payri, F., Torregrosa, A. and Chust, M., 1996. "Application of MacCormack Schemes to I.C. Engine Exhaust Noise Prediction". *Journal of Sound and Vibration*, Vol. 195, No. 5, pp. 757–773.

Toro, E.F., 1999. *Riemann Solvers and Numerical Methods for Fluid Dynamics*. Springer Berlin Heidelberg, Berlin, Heidelberg, 2nd edition.

White, F., 2011. *Fluid Mechanics*. McGraw Hill.

Winterbone, D.E. and Pearson, R.J., 2000. *Theory of Engine Manifold Design. Wave Action Methods for IC Engines.*, Vol. C. Professional Engineering Publishing.

7. RESPONSIBILITY NOTICE

The authors are the only responsible for the printed material included in this paper.